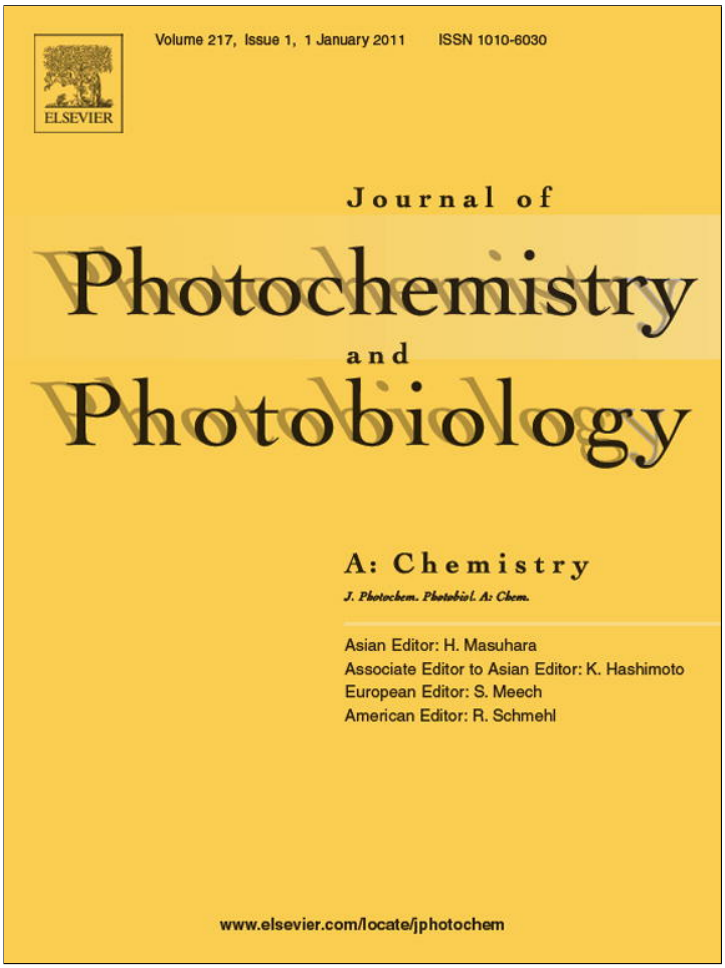

Journal of Photochemistry and Photobiology A: Chemistry 217 (2011) 87–99

Contents lists available at ScienceDirect

Journal of Photochemistry and Photobiology A: Chemistry

journal homepage: www.elsevier.com/locate/jphotochem

Photoinduced protonation and mechanical motion in the cyclodextrin cavity: Synthesis, structure and spectral properties of 4-(2-napthyl)pyridine and their pseudorotaxane complexes

Sergey P. Gromov[a,*], Valery B. Nazarov[b], Vitaly G. Avakyan[a], Marina V. Fomina[a], Artem I. Vedernikov[a], Lyudmila G. Kuz'mina[c], Tat'yana G. Vershinnikova[b], Natalia A. Lobova[a], Vladimir Yu. Rudyak[a], Michael V. Alfimov[a], Judith A.K. Howard[d]

[a] Photochemistry Centre, Russian Academy of Sciences, 7A-1 Novatorov str., 119421 Moscow, Russian Federation
[b] Institute of Problems of Chemical Physics, Russian Academy of Sciences, 142432 Chernogolovka, Moscow Region, Russian Federation
[c] N. S. Kurnakov Institute of General and Inorganic Chemistry, Russian Academy of Sciences, 31 Leninskiy prosp., 119991 Moscow, Russian Federation
[d] Chemistry Department, Durham University, South Road, Durham DH1 3LE, UK

ARTICLE INFO

Article history:
Received 29 June 2010
Received in revised form
21 September 2010
Accepted 25 September 2010
Available online 29 October 2010

Keywords:
Naphthylpyridine
β-Cyclodextrins
Inclusion complexes
Stability constants
Photoinduced protonation
Mechanical motion

ABSTRACT

The spontaneous and photoinduced protonation of 4-(2-naphthyl)pyridine (**1**) in solutions and in complexes with β-cyclodextrin (β-CD) and 2-hydroxypropyl-β-cyclodextrin (HP-β-CD) were studied by absorption and fluorescence spectroscopy. The structure and stability of the complexes ($\log K = 1.5–2.3$) of **1**, its protonated form **2**, and quaternized derivative, 1-methyl-4-(2-naphthyl)pyridinium perchlorate (**3**), with β-CD and HP-β-CD were studied by ^{1}H NMR. It was shown that irrespective of the solution pH, compound **1** resides in the cyclodextrin cavity. HP-β-CD better binds the neutral form of **1** than β-CD, while naphthylpyridinium salts have approximately equal binding affinity to both cyclodextrins. The structures of salt **3** and pseudorotaxane complex **1**@β-CD were determined by X-ray diffraction analysis. According to spectral data, pK_a of **1** in water is 5.12, which promotes protonation of nitrogen both in the ground state and in the excited state. As a consequence, the fluorescence spectrum exhibits only the protonated form with a lifetime of 15 ns. The addition of HP-β-CD to a solution of **1** results in inclusion complex **1**@HP-β-CD; simultaneously pK_a of **1** decreases to 4.62 and non-protonated form fluorescence (NFF) of **1** with a lifetime of 1.25 ns appears. Thus, the residence of **1** in the HP-β-CD cavity hampers its protonation in the excited state. From comparison of the initial regions of fluorescence of **1** in solution and in the HP-β-CD complex after pulse excitation, a mechanism for appearance of short-lived NFF of **1** was proposed. Quantum chemical simulation of the protonation and complexation of **1** in the presence of water was performed. On the basis of results, reversible photoinduced mechanical motion of **1** in the HP-β-CD cavity was suggested.

1. Introduction

The photoinduced intra and intermolecular proton transfer for organic compounds occurring in the excited state was previously studied in solutions (see, for example [1]). We showed [2] that in aqueous solution, 4-(2-naphthyl)pyridine (**1**) in the excited state adds a water proton to the nitrogen atom, and this gives rise to an intense fluorescence band (λ_{max} 475 nm), which undergoes a considerable bathochromic shift by 100 nm relative to the fluorescence maximum of **1** in aprotic solvents. Similar properties were also found for derivatives of **1** [3]. After the addition of β-cyclodextrin (β-CD) or 2-hydroxypropyl-β-cyclodextrin (HP-β-CD) to an aqueous solution of **1**, along with the protonated form fluorescence (PFF) of **1**, non-protonated form fluorescence (NFF) is also observed. This indicates that the formation of inclusion complexes of **1** with cyclodextrins hampers the protonation of **1** in the excited state. An obstacle to protonation can appear in the complex if the pyridine residue of **1** is immersed in the β-CD cavity, which is more hydrophobic than water. However, in molecule **1**, the naphthalene residue is more hydrophobic. Therefore, the formation of inclusion complex in which the naphthalene residue sits inside the cavity, while the hydrophilic pyridine residue is located outside the cavity and contacts the aqueous environment seems more likely a priori. Then the question arises of how the complexation hampers the protonation of **1**. In order to answer this question and to identify the processes involved in complexation, we carried out a comprehensive investigation of the properties of **1** and its derivatives.

* Corresponding author. Tel.: +7 495 935 0116; fax: +7 495 936 1255.
E-mail address: spgromov@mail.ru (S.P. Gromov).

1010-6030/$ – see front matter © 2010 Elsevier B.V. All rights reserved.
doi:10.1016/j.jphotochem.2010.09.022

The structure and stability of inclusion complexes formed by **1** and its protonated form **2** and quaternized form **3** with β-CD and HP-β-CD, which is better soluble in water than β-CD, were investigated by ^{1}H NMR spectroscopy. The structures of compound **3** and of complex **1** with β-CD were studied by X-ray diffraction. Using absorption and fluorescence spectra, photophysical processes in the complexes, resulting in NFF, were studied. For this purpose, the nanosecond fluorescence kinetics was measured, and the structure and the formation energy of the inclusion complexes of **1** with HP-β-CD and the role of water in the protonation of **1** were investigated by quantum chemical methods (DFT and PM3 calculations). In addition, the distance by which the "guest" molecule moves in the cyclodextrin cavity as a result of photoinduced protonation was estimated for the first time.

2. Experimental

2.1. Materials

Commercial hydroxypropyl-β-cyclodextrin (degree of substitution of 2-hydroxypropyl groups for the protons of the primary hydroxy groups of the macrocycle is 4.5) (Aldrich) and β-cyclodextrin (Cyclolab, Hungary) were used as received. Synthesis and structure of 4-(2-naphthyl)pyridine **1** were described earlier [4].

The obtained compounds were characterized by ^{1}H NMR spectroscopy and elemental analysis.

4-(2-Naphthyl)pyridinium perchlorate (**2**). A 70% solution of perchloric acid (30 μl) was added to naphthylpyridine **1** (21 mg, 0.1 mmol) dissolved in EtOH (1 ml). The reaction mixture was allowed to stand for 6 days at −6 °C. The precipitate was filtered off, washed with benzene, and recrystallized from a 1:1 benzene–EtOH mixture. The yield of **2** was 13 mg (42%), m.p. 236–238 °C.

^{1}H NMR (500 MHz, D_2O–MeCN-d_3 (4:1)) 30 °C, δ: 7.84–7.90 (m, 2H, H-6, H-7); 8.18–8.23 (m, 2H, H-5, H-8); 8.28–8.30 (m, 1H, H-3); 8.34 (d, 1H, *J* = 8.63 Hz, H-4); 8.52–8.53 (m, 2H, H-3′, H-5′); 8.71 (s, 1H, H-1); 8.94–8.95 (m, 2H, H-2′, H-6′). Anal. calcd. for $C_{15}H_{12}ClNO_4$: C, 58.93; H, 3.96; N, 4.58; found: C, 59.11; H, 3.79; N, 4.51.

1-Methyl-4-(2-naphthyl)pyridinium iodide. Methyl iodide (47 μl, 0.75 mmol) was added to a solution of **1** (100 mg, 0.5 mmol) in benzene (7 ml). The reaction mixture was allowed to stand at room temperature for 5 days. The resulting precipitate was filtered off and washed with benzene (3 × 5 ml) and pentane (3 × 5 ml). Yield 146 mg (86%), m.p. 215–216 °C (from EtOH).

^{1}H NMR (500 MHz, $CDCl_3$) 35 °C, δ: 4.67 (s, 3H, Me); 7.58–7.64 (m, 2H, H-6, H-7); 7.79 (d, 1H, *J* = 7.4, H-3); 7.88 (d, 1H, *J* = 7.4, H-4); 7.97–8.01 (m, 2H, H-5, H-8); 8.34–8.36 (m, 3H, H-1, H-3′, H-5′); 9.24–9.26 (m, 2H, H-2′, H-6′). Anal. calcd. for $C_{16}H_{14}IN$: C, 55.35; H, 4.06; N, 4.03; found: C, 54.91; H, 4.04; N, 3.89.

1-Methyl-4-(2-naphthyl)pyridinium perchlorate (**3**). A 70% solution of perchloric acid (30 μl) was added to 1-methyl-4-(2-naphthyl)pyridinium iodide (35 mg, 0.1 mmol) dissolved in MeOH (3 ml). The reaction mixture was allowed to stand for 24 h at room temperature. The resulting precipitate was filtered off and recrystallized from MeOH. The yield of **3** was 17 mg (52%), m.p. 199–201 °C.

^{1}H NMR (500 MHz, D_2O–MeCN-d_3 (4:1)) 30 °C, δ: 4.52 (s, 3H, Me); 7.85–7.91 (m, 2H, H-6, H-7); 8.18–8.22 (m, 2H, H-5, H-8); 8.29–8.30 (m, 1H, H-3); 8.34 (d, 1H, *J* = 8.63, H-4); 8.58–8.59 (m, 2H, H-3′, H-5′); 8.75 (br.s, 1H, H-1); 8.92–8.94 (m, 2H, H-2′, H-6′). Anal. calcd. for $C_{16}H_{14}ClNO_4$: C, 59.91; H, 4.71; N, 4.37; found: C, 59.84; H, 4.56; N, 4.31.

2.2. Methods

Melting points were measured on a Mel-Temp II instrument. Elemental analyses were carried out at the Laboratory of Microanalysis of the A. N. Nesmeyanov Institute of Organoelement Compounds (Russian Academy of Sciences, Moscow).

2.2.1. X-ray diffraction experiments

The crystals of compound **3** were prepared by slow evaporation of its solution in MeCN at room temperature. The crystals of complex **1**@β-CD were obtained by slow evaporation of an equimolar mixture of components in a MeCN–water mixture at room temperature. The single crystals were mounted on a Bruker SMART-CCD diffractometer under a cooled nitrogen stream (*T* = 120.0(2) K) and intensities of experimental reflections were measured (Mo-K_α radiation, λ = 0.71073 Å, graphite monochromator, ω-scan mode). The structures were solved by direct methods. In complex with β-CD, one of two crystalographically independent molecule **1** is disordered over two positions with the occupancy ratio of 0.54:0.46. The structures were refined in the full-matrix anisotropic approximation on F^2 for non-hydrogen atoms except for the atoms of the disordered molecule **1** that were refined isotropically. The primary hydroxy groups, O(15C) and O(25C), in both independent β-CD molecules were found to be disordered over two positions with occupancy ratios of 0.61:0.39 and 0.72:0.28. In the crystal unit cell of **1**@β-CD, 24 independent solvation water molecules with full or partial position occupancies were detected. Note that difference Fourier syntheses revealed numerous minor electron density peaks around the basis elements of the crystal; however, attempts to attribute these peaks to water molecules with incomplete position occupancies failed. Thus, many crystal components of complex **1**@β-CD are substantially disordered, especially one of the independent molecules **1** and the solvation shell. This is a typical feature of loose supramolecular architectures based on cyclodextrins. For this reason the accuracy of X-ray experiments for such species are often not very high. When refining this structure, we used a number of geometric restraints (AFIX 66, AFIX 116, SADI, ISOR commands). The positions of hydrogen atoms at carbons were calculated geometrically and refined in the isotropic approximation for structure **3** and using a "riding" model for complex **1**@β-CD. The hydroxyl hydrogen atoms of β-CD and solvate water molecules were not located. All the calculations were carried out using the SHELXTL-Plus program package [5]. The crystal parameters and X-ray experiment details are summarized in Table 1. The atom coordinates and other experimental data are deposited with the Cambridge Crystallographic Data Centre (CCDC)[1] under the numbers 781945 (**3**) and 781944 (**1**@β-CD).

2.2.2. ^{1}H NMR spectroscopy measurements and titration

The ^{1}H NMR spectra were recorded on a Bruker DRX500 spectrometer in $CDCl_3$ and a D_2O–MeCN-d_3 mixture (4:1) at 30 °C with the solvent or the HOD signal as the internal standard (δ_H 7.27 or 4.70, respectively). The ^{1}H–^{1}H COSY and ROESY two-dimensional homonuclear spectra were used to assign the proton signals and determine the structure of the complexes. 2D-experiments were carried out using standard parameters included in the Bruker software package. The mixing time in the ROESY experiment was 300 μs. In ^{1}H NMR titration, the compositions and stability constants of the complexes of compounds **1–3** with cyclodextrins were determined by analyzing the changes in the positions of the proton signals ($\Delta\delta_H$) of the substrate depending on the concentration ratio of cyclodextrin and the substrate. The cyclodextrin

[1] CCDC, 12 Union Road, Cambridge CB21EZ, UK (fax: (+44) 1223 33 6033; e-mail: deposit@ccdc.cam.ac). A copy of the data is available from the authors.

Table 1
Crystal data and structure refinement for **3** and **1**@β-CD.

Compound	**3**	**1**@β-CD·9.13H_2O
Formula	$C_{16}H_{14}ClNO_4$	$C_{57}H_{99.25}NO_{44.13}$
Molecular weight (g mol^{-1})	319.73	1504.62
Crystal system	Monoclinic	Monoclinic
Space group	$P2_1/n$	$P2_1$
a (Å)	7.2307(3)	15.3332(19)
b (Å)	10.6633(4)	31.700(4)
c (Å)	19.3911(7)	15.540(2)
β (°)	97.973(2)	102.459(5)
V (Å^3)	1480.66(10)	7375.6(17)
Z	4	4
d_{cal} (g mL^{-1})	1.434	1.355
F(0 0 0)	664	3205
μ (mm^{-1})	0.276	0.118
Crystal size (mm^3)	0.36 × 0.26 × 0.14	0.22 × 0.10 × 0.06
θ range (°)	2.12–28.99	1.34–25.00
h k l range	$-9 \le h \le 9$, $-13 \le k \le 14$, $-19 \le l \le 26$	$-18 \le h \le 18$, $-37 \le k \le 37$, $-18 \le l \le 18$
Reflections collected/unique [R(int)]	8966/3802 [0.0376]	56521/25892[0.2694]
Completeness (%) [to θ/°]	96.6 [28.99]	100.0 [25.00]
Data, restraints, parameters	3802, 0, 255	25892, 472, 1822
Goodness-of-fit on F^2	1.042	0.853
R_1, wR_2 [$I > 2\sigma(I)$]	0.0488, 0.1065	0.1169, 0.2464
R_1, wR_2 [all data]	0.0744, 0.1147	0.3370, 0.3165
Largest diff. peak, hole (ē Å^{-3})	0.265, −0.315	0.924, −0.414

concentration was varied in the range from 0 to 3×10^{-3} mol L^{-1}, while the overall concentration of **1–3** did not change remaining equal to $\sim 1 \times 10^{-3}$ mol L^{-1}. The $\Delta\delta_H$ values were measured to an accuracy of 0.001 ppm with correction for MeCN-d_2 signal shift. The stability constants of the complexes were calculated using the HYPNMR program [6]; the logarithms of the constants are summarized in Table 2.

2.2.3. Optical spectroscopy measurements

Complexes of **1** with cyclodextrins for spectral measurements were prepared by adding the substrate to heated (50 °C) aqueous solutions of β-CD and HP-β-CD and kept for 24 h or longer at room temperature prior to investigation. The concentration of **1** in solutions was in the range of 10^{-6}–10^{-4} mol L^{-1} and cyclodextrin concentration was 5 10^{-3} mol L^{-1}. Doubly distilled water, hexane purified by column chromatography on silica gel followed by distillation, and commercial Reachim Grade-F acetonitrile (water content < 0.01%) were used as solvents.

The absorption spectra were measured on a Specord–M40 spectrophotometer. The fluorescence spectra were recorded on Elumin–2M and Perkin Elmer LS55 spectrofluorimeters. The fluorescence kinetics and lifetime were measured on a Fluotime 200 fluorescence spectrometer (PicoQuant GmbH). The pK_a values were obtained from UV/vis absorption spectra recorded at different pH of the solution. The fluorescence quantum yield, φ_f, was measured using anthracene with $\varphi_f = 0.3$ (in ethanol) as the standard [7].

2.2.4. Quantum chemical calculations

The quantum chemical calculations with full geometry optimization for all of the compounds and complexes were carried out by semiempirical PM3 method with a standard set of parameters [8] (PC GAMESS program by A.A. Granovsky, M.V. Lomonosov Moscow State University). The heats of formation, ΔH_f, the binding energies of the complex components, E_{bind}, and the insertion energies of naphthylpyridine with allowance for water were determined (**1n** and **1p** mean that naphthylpyridine in inserted into the HP-β-CD cavity with the naphthalene or pyridine residue, respectively). The E_{bind} values were found as the difference between ΔH_f of the optimized complex and the sum of ΔH_f of its components.

The protonation of **1** in the ground and excited states was calculated using the TDDFT method with the PBE exchange correlation functional implemented in the Priroda 6 program package [9].

The exact structure of 2-hydroxypropyl-β-cyclodextrin is unknown [10]. This is due to the fact that the preparation of HP-β-CD by treatment of β-cyclodextrin with propylene oxide in alkaline medium gives an unseparable mixture of alkylation products in which hydroxypropyl groups substitute in a random pattern the hydrogen atoms of the OH groups; in more alkaline medium, mainly primary O(6) groups are replaced [10]. As the initial structure for HP-β-CD geometry optimization, we used a symmetric β-CD model (C_7 symmetry group) in which all seven primary hydroxy groups were substituted by 2-hydroxypropyl groups taken in such a conformation that all OH groups were oriented outward with respect to the hydrophobic cavity, i.e., to the aqueous medium, thus ensuring the highest solubility of HP-β-CD. The HP-β-CD structure obtained upon full optimization, which also had C_7 symmetry, was then used to construct the models of inclusion complexes. Note that the model with seven 2-hydroxypropyl groups, $CH_2CH(OH)CH_3$, located at the narrow HP-β-CD portal has the deepest cavity as compared with the structures in which not all of the hydrogen atoms of primary hydroxy groups have been replaced by 2-hydroxypropyl groups. Thus, the E_{bind} values found for this HP-β-CD model can be considered as the upper limit of the complex formation energy. Since the substitution is random [10], in this work we calculated also a less regular model (HP-β-CD (4p, 3s)) in which four $CH_2CH(OH)CH_3$ groups have replaced the primary OH groups and three $CH_2CH(OH)CH_3$ groups have replaced the secondary OH groups (two O(2) and one O(3)). This was done to find out the change in the heat of formation for a free HP-β-CD molecule in which secondary OH groups would be replaced by the $CH_2CH(OH)CH_3$ groups. The results of calculations of the molecules and complexes are summarized in Table 3.

Table 2
Stability constants of the complexes of compounds **1–3** with β-CD and HP-β-CD[a].

Compound	log K[b]		
	1	**2**	**3**
β-CD	1.9	1.7	1.6
HP-β-CD	2.3	1.7	1.5

[a] ^{1}H NMR-titration in D_2O–MeCN-d_3 (4:1), 30 °C.
[b] K = [**1**(**2**,**3**)@CD]/([**1**(**2**,**3**)]·[CD]), L mol^{-1}; error of determination of the constants is ±30%.

Table 3
Heats of formation and relative energies of compounds and complexes calculated by PM3, kcal mol^{-1}.

Compound and complexes	ΔH_f[a]	E_{bind}[b]	ΔE_{bind}[d]
H_2O	−53.4		
$5H_2O$	−291.0	−23.9[c]	
HP-β-CD	−1792.2		−12.0[e]
HP-β-CD (4p,3s)	−1780.2		0
$5H_2O$@HP-β-CD	−2090.9	−7.7	
1	71.7		
1·$5H_2O$	−215.2		−25.7[f]
1$H^+OH^-·4H_2O$	−189.5		0
1p·$5H_2O$@HP-β-CD	−2020.4	−13.0	−5.3[g]
1n·$5H_2O$@HP-β-CD	−2019.1	−11.7	−5.3[g]
1p$H^+OH^-·4H_2O$@HP-β-CD	−1996.1	−14.4	24.3[h]
1n$H^+OH^-·4H_2O$@HP-β-CD	−1997.4	−15.7	22.0[h]

[a] Calculated heat of formation.
[b] Binding energy of the guests with HP-β-CD.
[c] Formation energy of the pentahydrate cluster.
[d] Relative energies of:
[e] Two HP-β-CD structures,
[f] Naphthylpyridine pentahydrate and its ion pair,
[g] Inclusion complexes **1**·$5H_2O$@HP-β-CD and $5H_2O$@HP-β-CD,
[h] Binding energies of **1**·$5H_2O$@β-CD and inclusion energies of **1** ion pair in HP-β-CD.

3. Results and discussion

3.1. Synthesis of compounds *1–3*

In order to investigate the structure and the stability of complexes of 4-(2-naphthyl)pyridine **1** with β-CD and HP-(-CD, we synthesized 4-(2-naphthyl)pyridine **1** and its derivatives, naphthylpyridinium perchlorate **2** and 1-methyl-4-(2-naphthyl)pyridinium perchlorate **3**. The synthesis of compound **1** was described in our previous publication [4]. The naphthylpyridinium perchlorate **2** was obtained in 42% yield by the reaction of **1** with an excess of 70% perchloric acid in ethanol. 1-Methyl-4-(2-naphthyl)pyridinium perchlorate **3** was obtained by quaternization of **1** with methyl iodide followed by the anion exchange with the perchlorate ion on treatment with perchloric acid in methanol (Scheme 1). The yield at the last stage was 52%.

3.2. X-ray diffraction study of *3* and *1*@β-CD

Compound **3** was obtained as a single crystal and studied by X-ray diffraction. The structure of the independent components of the crystal unit cell is shown in Fig. 1. The bond length distribution in **3** is typical of the naphthalene and quaternized pyridine residues. The length of the C(3)–C(6) bond connecting these residues equals 1.485(2) Å. The organic cation adopts a near planar conformation, which is best suited for effective conjugation throughout the whole chromophore: the dihedral angle between the naphthalene and pyridine planes is only 3.9°. However, this conformation is, most likely, a consequence of the packing mode of organic cations, because our calculations of the ground-state protonated naphthylpyridine **2** demonstrated that the aromatic residues are rotated through 22° (see below). Fig. 2 shows a

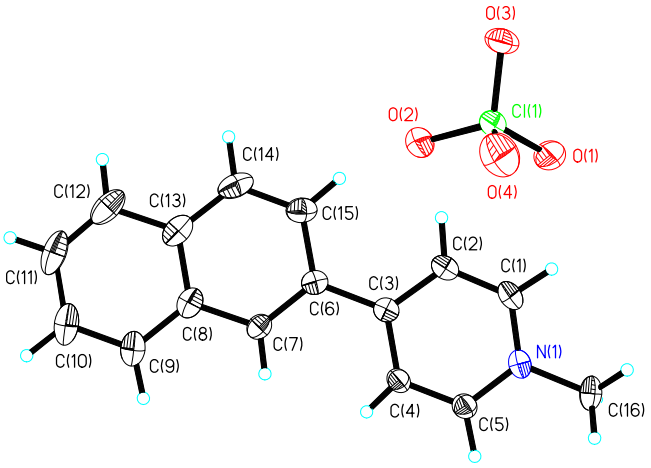

Fig. 1. Structure **3**. All non-hydrogen atoms are shown at 50% probability of their anisotropic thermal parameters.

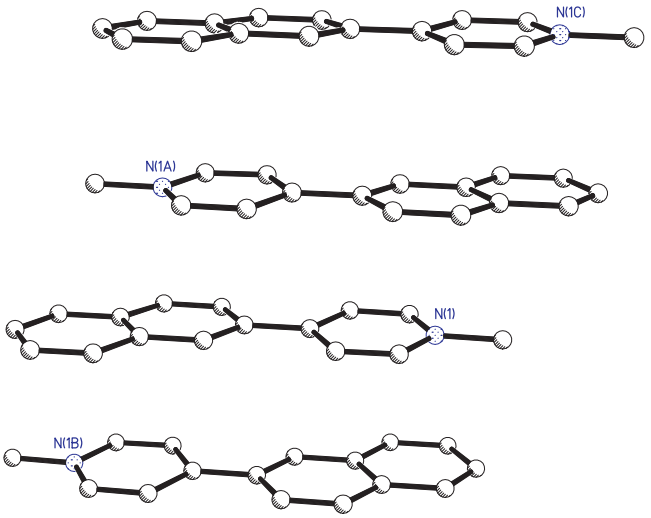

Fig. 2. Stacking of cations **3**. Hydrogen atoms are omitted for clarity.

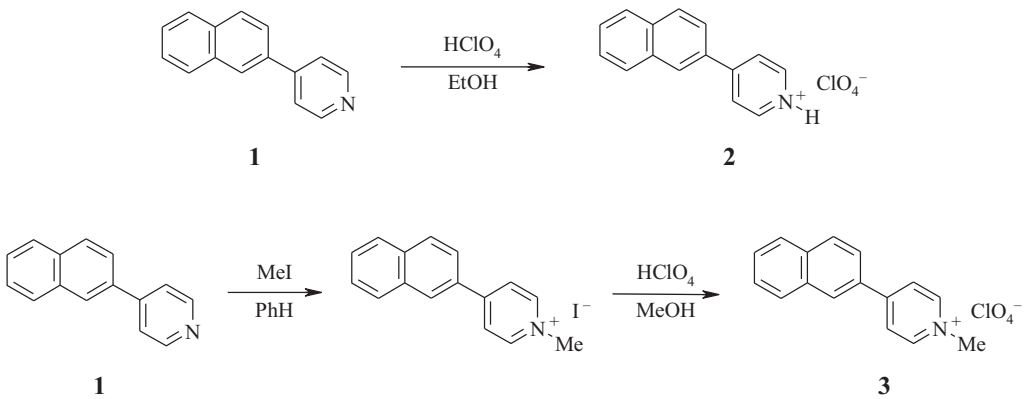

Scheme 1. Synthesis of the protonated form **2** and quaternized derivative **3** of 4-(2-naphthyl)pyridine.

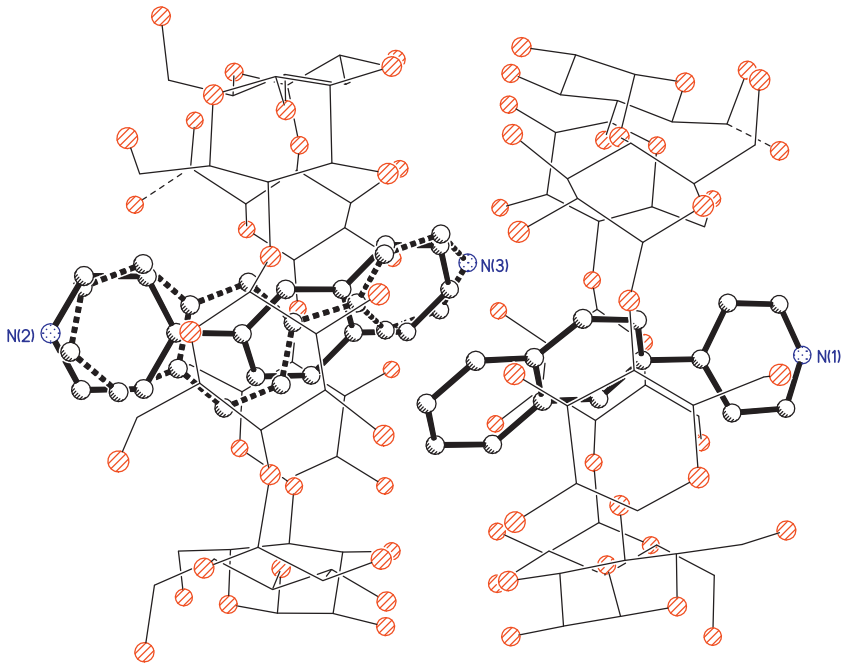

Fig. 3. Structure of two independent complexes **1**@β-CD in the side projection. All solvate water molecules and hydrogen atoms are omitted for clarity. One of two independent molecules **1** is disordered over two positions.

fragment of stack packing formed by cations in the crystal of compound **3**. It can be seen that cations are located one above another in the head-to-tail pattern, thus ensuring high degree of projection of their conjugated systems onto one another. Both interplanar distances, N(1),C(1)...C(16)/N(1A),C(1A)...C(16A) and N(1),C(1)...C(16)/N(1B),C(1B)...C(16B), are approximately 3.4 Å, which implies effective stacking interactions between the neighbouring cations in the stack.

We also managed to obtain crystals of compound **1** complex with β-CD as fine colourless prisms. The quality of these crystals proved to be poor due to pronounced disorder of the components; however, it can be stated with confidence that the found structural motif and the overall geometry of complexes are sufficiently correct to discuss the characteristic features of the mutual arrangement of components. The main components of the crystal unit cell, namely, two independent complexes **1**@β-CD, are shown in Fig. 3. Two

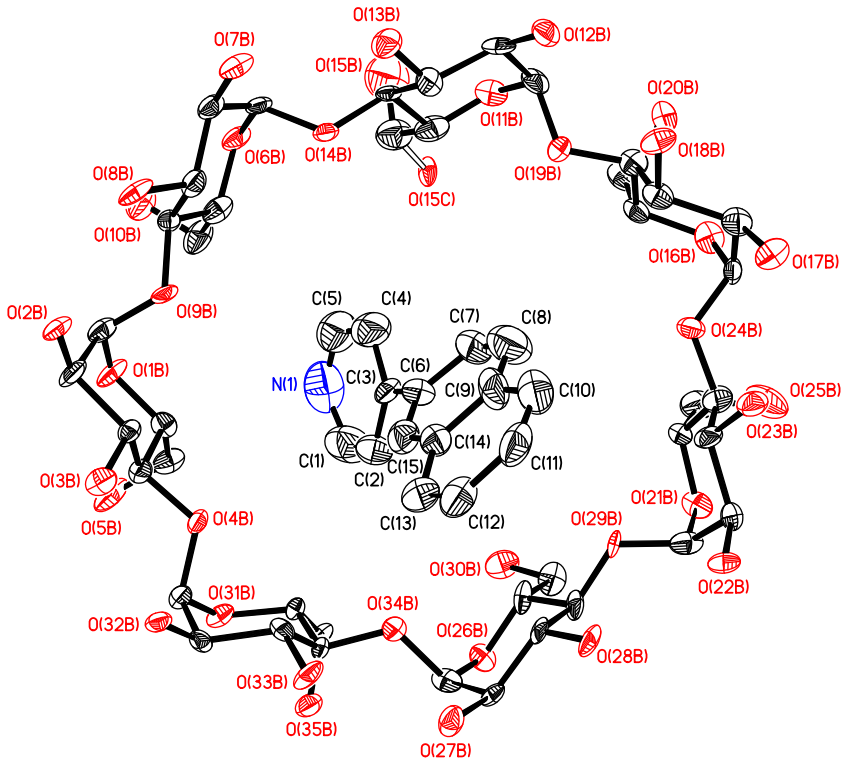

Fig. 4. Structure of one of two independent complexes **1**@β-CD in the front projection. All atoms are shown at 30% probability of their anisotropic thermal parameters. Hydrogen atoms are omitted for clarity.

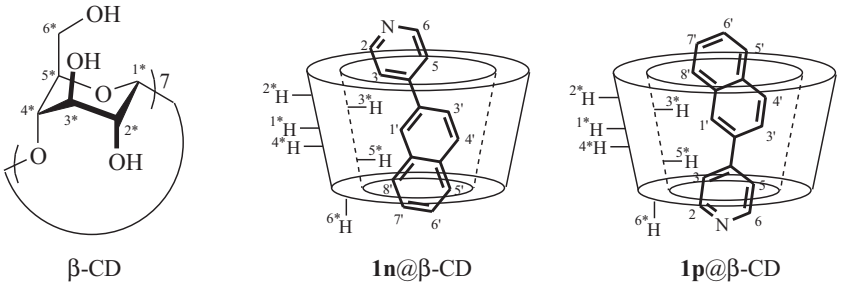

Scheme 2. Structure of β-CD and two possible complexes **1**@β-CD.

independent cyclodextrin molecules are arranged with their wide portals toward each other to form head-to-head dimer $[\beta\text{-CD}]_2$ the components of which are linked by numerous intermolecular hydrogen bonds between secondary hydroxy groups. This is indicated by the O···O distances between the oxygen atoms of the secondary hydroxy groups of the dimer components, which vary in the 2.73–3.14 Å range. Each independent cyclodextrin molecule accommodates one naphthylpyridine molecule, its terminal fragments protruding slightly beyond the cyclodextrin cavity on both sides, thus forming pseudorotaxane complexes **1**@β-CD. The key difference between the two independent complexes is the disordered position of the guest molecule in one of them. In one of the complexes, the pyridine residue of molecule **1** is located in the narrow section of the cone-like cyclodextrin cavity, whereas in the other complex, the narrow section is occupied by either pyridine or naphthalene fragment. Note that even the "ordered" naphthylpyridine **1** molecule is not securely fixed inside the β-CD. This conclusion is based on large amplitudes of the thermal anisotropic motion observed for the non-hydrogen atoms of this molecule as compared with analogous characteristics of the host molecule (Fig. 4). This fact attests to free position of the relatively small guest molecule in the β-CD cavity and the possibility of its easy motion inside the cavity. All molecules **1** acquire a non-planar conformation: the dihedral angles between the pyridine and naphthalene ring planes, N(1)C_5/C(6)...C(15), N(2)C_5/C(6′)...C(15′), and N(3)C_5/C(6″)...C(15″), are 45.3, 32.3, and 34.5°, respectively.

The $[\beta\text{-CD}]_2$ dimer has a common, fairly large cavity, in which the planar fragments of two independent molecules **1** are involved in rather effective stacking interactions. Owing to the above-described disorder of one of the guest molecules, the stacking interactions occur either between two naphthalene fragments (the C(6)...C(15)/C(6′)...C(15′) dihedral angle is 4.2°, the interplanar spacing is ~3.7 Å) or between the naphthalene and pyridine fragments (the C(6)...C(15)/N(3)C_5 dihedral angle is 6.3°, the interplanar spacing is ~3.8 Å). Thus, the dimeric complex $[\mathbf{1}@\beta\text{-CD}]_2$, whose existence was assumed in our previous work based on calculations [2], was actually found in the crystal.

3.3. ^{1}H NMR spectroscopy studies

NMR spectroscopy is extensively used to establish the structure and determine the stability of various supramolecular complexes in the solution, in particular, to determine the mode of inclusion of the guest molecule into the cyclodextrin cavity, the complexation stoichiometry, and the stability of these complexes [11]. We studied mixtures of compounds **1–3** with β-CD and HP-β-CD using 2D NMR spectroscopy and ^{1}H NMR titration. Preliminary experiments have shown that to attain a hydrophobic substrate concentration needed to carry out the NMR experiment (~1×10^{-3} mol L^{-1} and more), it was necessary to use a water–organic solvent mixture. In particular, we chose the D_2O–MeCN-d_3 mixture (4:1) in which the solubility of most hydrophobic compound **1** was about 1.6×10^{-3} mol L^{-1}, and the solubility of the studied cyclodextrins was not less than 6×10^{-3} mol L^{-1} at 30 °C.

It is known that the β-CD macrocycle is built of seven α-glucopuranose units linked to one another through positions 1* and 4* (Scheme 2).

This coupling results in the formation of a truncated-cone-like cavity with two non-equivalent portals in which only protons in positions 3* and 5* point inside the cavity. Fig. 5 shows a fragment of the ROESY spectrum of a mixture of **1** and β-CD, demonstrating the intermolecular interactions. It can be seen that relatively weak cross-peaks are observed for through-space interactions of most of the substrate protons with the "internal" H-3*, H-5* protons and the methylene H-6* protons of cyclodextrin. This implies that the hydrophobic molecule **1** is located in the lipophilic cavitand cavity, in addition, the spectral pattern attests to implementation of both possible modes of arrangement of the unsymmetrical guest molecule within β-CD. This is in good agreement with X-ray diffraction data (see Section 3.2).

A similar pattern of intermolecular interactions is observed in the ROESY spectra of mixtures of ionic compounds **2**, **3** with β-CD. The slight distinction from the ROESY spectrum of a neutral **1**-β-CD mixture consists in lower intensity of cross-peaks corresponding to interactions between the pyridine H-3 and H-5 protons of compounds **2**, **3** and the "internal" cyclodextrin protons. This implies that the hydrophilic positively charged pyridine residue in complexes **2**(**3**)@β-CD is more "protruded" to the water–acetonitrile medium than this is observed in complex **1**@β-CD.

Due to incomplete replacement of the protons of primary hydroxy groups by 2-hydroxypropyl groups in HP-β-CD, its ^{1}H NMR spectrum is a set of highly broadened lines. The ROESY spectra of mixtures of compounds **1–3** and HP-β-CD exhibit very weak cross-peaks corresponding to intermolecular interactions that are

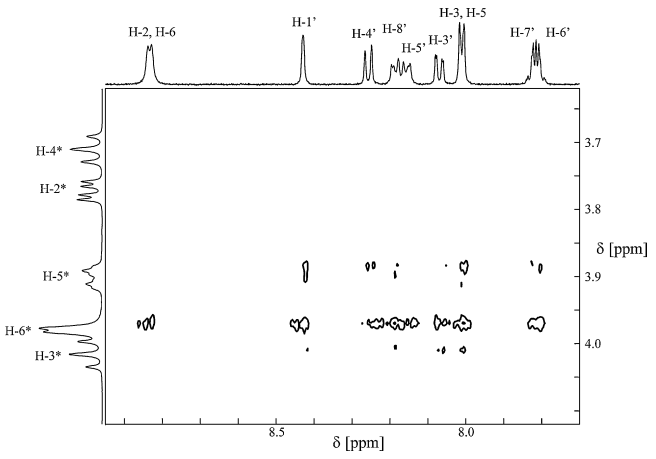

Fig. 5. Fragment of the ROESY spectrum of a mixture of **1** ($C_1 = 1.6 \times 10^{-3}$ mol L^{-1}) and β-CD ($C_{\beta\text{-CD}} = 6 \times 10^{-3}$ mol L^{-1}), D_2O–MeCN-d_3 (4:1), 30 °C.

difficult to interpret. However, the position of these cross-peaks (at about 3.9–4.0 ppm for aliphatic protons) indicates, most likely, the formation of inclusion complexes **1**(**2**,**3**)@HP-β-CD similar in their structure to β-CD complexes.

The stability of complexes **1–3** with cyclodextrins (CD) was determined quantitatively by ^{1}H NMR titration. It is noteworthy that mixing of the components causes relatively small and oppositely directed shifts of proton signals of both the substrate and cyclodextrin ($\Delta\delta_H$ up to 0.10 ppm). This is a usual behaviour of cyclodextrin-based supramolecular systems [11]. The variation of the proton chemical shifts of the substrate vs. the change in the CD to substrate concentration ratio was well described by a model taking into account only one equilibrium:

$$\mathbf{1}(\mathbf{2},\mathbf{3}) + \mathrm{CD} \overset{K}{\rightleftarrows} \mathbf{1}(\mathbf{2},\mathbf{3})@\mathrm{CD} \quad (1)$$

where K is the stability constant of the 1:1 complex, L mol^{-1}. The found stability constants, log K, are presented in Table 2.

The data of Table 2 show that the stability of complexes formed by compound **1** with β-CD or HP-β-CD decreases on going from aqueous solution to a water–acetonitrile mixture (in water, log K is 3.30 and 3.53, respectively [3]). This, undoubtedly, reflects the decrease in the hydrophilic nature of the medium, which interferes with the retention of the hydrophobic substrate in the macrocycle cavity. The log K values decrease in parallel, i.e., complex **1**@β-CD remains less stable than **1**@HP-β-CD due to the more pronounced lipophilicity of the cavity of the latter cyclodextrin having hydrophobic substituents at the primary OH groups. In the case of ionic naphthylpyridine derivatives **2**, **3**, the stabilities of complexes with both cyclodextrins become approximately equal (log K = 1.5–1.7), and they are lower than the stability of complexes formed by neutral **1**. This also reflects the increase in the hydrophilicity of the substrate on passing from the neutral to the cationic form, resulting in its lower affinity for the lipophilic cyclodextrin cavity. Note, however, that this increase in the hydrophilicity of **2** and **3** does not induce complete destruction of inclusion complexes, perhaps, owing to the hydrophobic nature of the naphthalene fragment in all of the studied substrates.

3.4. Electronic absorption (UV/vis) spectra

The spectra of **1** depend little on the solvent used. However, in aqueous solutions at low pH, the nitrogen atom is protonated, and the absorption spectrum undergoes a substantial bathochromic shift (see Fig. 6). Processing of the absorption spectra of aqueous solutions of **1** with different perchloric acid contents gave pK_a = 5.18. This value is very similar to the experimental value of 5.21 for pyridine [12].

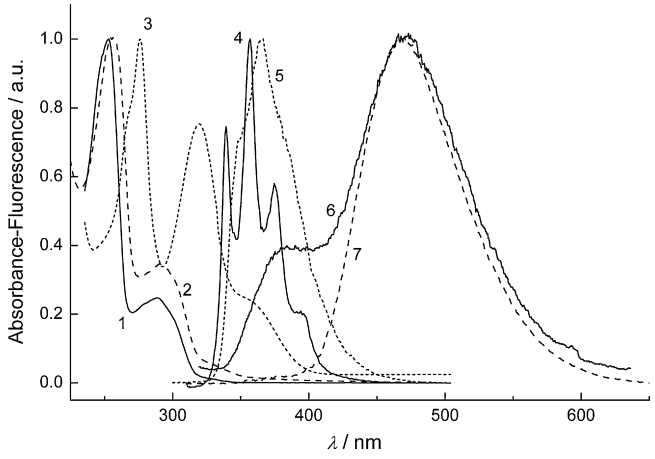

Fig. 6. Normalized (1–3) UV/vis absorption and (4–7) fluorescence spectra of **1** in (1,4) hexane, (2,7) water, (5) MeCN, and of (6) a mixture of **1** with HP-β-CD in water and (3) with added $HClO_4$.

$$\mathbf{1} + H_2O \rightarrow \mathbf{1}{\cdot}H_2O \xrightarrow{h\nu} \mathbf{1}^*{\cdot}H_2O \rightarrow \mathbf{1}{\cdot}H^+{}^* \,\|\, OH^- \rightarrow \mathbf{1}{\cdot}H_2O + h\nu_1\ (475\ \mathrm{nm})$$

Scheme 3. Photoinduced protonation and fluorescence of **1** in aqueous solution.

When the solution is stored in air, protonation of **1** is fairly effective, apparently, due to the appearance of carbonic acid in water, as follows from the change in the absorption spectrum.

A freshly prepared neutral aqueous solution of **1** contains also the hydrated form of **1**, which is responsible for weak absorption in a longer-wavelength region as compared with the spectrum of **1** in hexane. A similar spectral change was noted for aqueous solution of 4,4′-bipyridine [13].

The addition of HP-β-CD, which is more readily soluble than β-CD, to a solution of **1** also has little influence on the absorption spectrum of the non-protonated form. However, while the protonated form of **1** was partly formed in the presence of carbon dioxide, in the case of HP-β-CD, its fraction was much smaller. This implies that after the insertion into the HP-β-CD cavity, deprotonation of **1** takes place. A similar effect was found for complex **1**@β-CD in water.

3.5. Fluorescence spectra and lifetimes of *1* in solutions

Fig. 6 (4–6) shows the fluorescence spectra of **1** in different solvents. In the spectrum of a neutral aqueous solution, the broad band with a maximum at 475 nm corresponds to protonated **1** formed in the excited state [2]. Scheme 3 reflects these processes.

The fluorescence quantum yield for **1** in water is nearly unity. The fluorescence lifetime after purging the aqueous solution with argon is 15 ± 0.1 ns, and in the presence of perchloric acid added, this value is 14.7 ± 0.1 ns. In both cases, the fluorescence decay is described by a monoexponential dependence. In hexane and in MeCN, the fluorescence quantum yield of the non-protonated form of **1** equals 0.09 ± 0.02 and 0.7 ± 0.15, respectively.

In aprotic solvents, the fluorescence maximum of **1** is shifted hypsochromically by approximately 100 nm compared to the aqueous solution. In non-polar hexane, the NFF band of **1** clearly exhibits the electron-vibrational structure, whereas in polar MeCN, it is poorly pronounced (Fig. 6).

3.6. Spectral properties and fluorescence lifetimes of *1* in the complex with HP-β-CD

The addition of β-CD or HP-β-CD to an aqueous solution of **1** leads to the formation of inclusion complexes, which results in considerable changes in the fluorescence spectra of **1** [2,3]. The main effect is appearance of the non-protonated form fluorescence (NFF) of **1** with a maximum at 375 nm (Fig. 6, spectrum 6) and simultaneous decrease in the protonated form fluorescence (PFF) at 475 nm. In addition, due to the reduced protonation, the pK_a value of complex **1** with HP-β-CD becomes equal to 4.62, which gives rise to NFF. It is clear that NFF can exist only provided that the protonation of **1** in the excited state would be prevented by the formation of the inclusion complex.

Depending on what fragment of molecule **1**, naphthalene or pyridine one, resides inside the cavity, two types of inclusion complexes of **1** with HP-β-CD are possible. At the first glance, the structure in which the more hydrophobic naphthalene fragment is wholly located inside the cavity, while the more hydrophilic pyridine fragment is partly outside the cavity and can contact with the aqueous phase should be preferred. However, the experimental fact that the addition of HP-β-CD hampers protonation indicates that

Table 4
Fluorescence lifetimes of **1**–**3** in solutions and in the complexes with HP-β-CD.

Sample	λ_{obs} (nm)	τ (ns)	Relative amplitude
1@HP-β-CD	370 (NFF)	1.25 ± 0.3	6
		4.87 ± 0.13	1
	490 (PFF)	17.1 ± 0.1	3
		6.2 ± 0.4	1
1 – H_2O	470	15 ± 0.1	Monoexponent
1 – MeCN	370	9.5 ± 0.05	Monoexponent
2@HP-β-CD	480	16.1 ± 0.1	Monoexponent
2 – H_2O	480	14.7 ± 0.03	Monoexponent
2 – MeCN	480	13.3 ± 0.03	Monoexponent
3@HP-β-CD	480	15.32 ± 0.05	Monoexponent
3 – H_2O	480	14.55 ± 0.05	Monoexponent
3 – MeCN	480	12.73 ± 0.03	Monoexponent

the pyridine fragment of **1** can also be located inside the cyclodextrin cavity and, most likely, that these types of complexes occur in equilibrium in line with the NMR and X-ray diffraction data. Otherwise, i.e., if the naphthalene residue is located fully inside the cavity and the pyridine residue is fully outside, the formation of the inclusion complex could hardly affect protonation. Therefore, the protonation rate of **1** in the excited state is determined by the position of the pyridine residue of **1** inside the HP-β-CD cavity.

For more detailed investigation of this phenomenon, we measured the fluorescence lifetimes of **1–3** in solutions and in the complex with HP-β-CD. The fluorescence of **1** was excited at 280 nm, and that of the cationic forms of **1** also at 375 nm. The results are summarized in Table 4. The decays of fluorescence of complexed **1** observed for NFF of **1** at 370 nm and for PFF of **1** at 490 nm followed a biexponential pattern, whereas in solutions of **1**, only monoexponential decays were observed. The interpretation of the fluorescence lifetimes presented in Table 4 was based on conclusion stating the existence of two types of complexes differing in the arrangement of the pyridine residue of **1** relative to the HP-β-CD cavity.

Immediately after pulse excitation of **1**, if no protonation of the nitrogen atom takes place, NFF is always observed. However, in aqueous solution of **1**, no NFF is recorded in the nanosecond time scale but only the stationary PFF spectrum is observed, indicating high protonation rate of **1** in the excited state. According to quantum chemical calculations (see Section 3.7), after the formation of complex **1n**@HP-β-CD in which the pyridine residue of **1** occurs outside the HP-β-CD cavity, it still has a somewhat limited contact with water, as the approach of water molecule from the cyclodextrin side is hampered. Therefore, the possibility of existence of the NFF with a short lifetime of 1.25 ns appears (Fig. 7 shows only the five water molecules that hydrate the pyridine nitrogen and were included in calculations).

For the complex in which the pyridine residue of **1** is located inside the HP-β-CD cavity (see Fig. 7a), the protonation of **1** after excitation is appreciably limited, i.e., the access for a proton from the aqueous phase is impeded and a proton transfer from the water pentamer is apparently less effective, as the surrounding four water molecules may not suffice for stabilizing the protonated form, which is a $C_{15}H_{11}N^+$–H. . .$^-$OH ion pair (Fig. 7b, see Section 3.7). Therefore, the NFF lifetime in this complex increases becoming equal to 4.87 ns but it is shorter than that in MeCN where protonation of **1** in the excited state competing with the NFF is absent. Hence, the NFF lifetimes are determined by the rate of protonation of **1** in the excited state, which depends on the structure of the inclusion complexes formed.

Following pulse excitation, PFF of complexed **1** (curve 2 in Fig. 8) appears after a noticeable delay with respect to the NFF (curve 1 in Fig. 8) or to the NFF in anhydrous MeCN (curve 3 in Fig. 8) where no protonation of **1** in the excited state takes place. In the initial segments of the curves reflecting the kinetics of PFF building-up and NFF decay in the complex, one can see the opposite courses of the curves, indicating that these processes are related. This means that PFF actually appears as a result of protonation of **1** in the excited state and thus competes with NFF and determines its lifetime.

Note that if the pyridine residue of **1** is located outside the HP-β-CD cavity, then after the formation of the protonated form of **1** in the excited state, in view of the aqueous environment of the nitrogen atom, one can expect that the PFF lifetime would be of the same order as the time found for the aqueous solution of **1**. Therefore, the value τ 17.1 ns should be assigned to the PFF of complex **1n**@HP-β-CD.

From comparison of the fluorescence spectra of naphthylpyridine derivative in the complex with HP-β-CD and in aprotic MeCN solvent, it was concluded that the polarities of MeCN and the HP-β-CD cavity do not differ much [3]. In anhydrous MeCN, the fluorescence lifetimes of **2** and **3**, which are ionic derivatives of **1**, are 13.3 and 12.73 ns, respectively, which is shorter than in water. Therefore, for the excited state of the complex of protonated **1** having the pyridine fragment inside the cavity, a shorter PFF lifetime should be expected compared to that in water. This corresponds to the time of 6.2 ns. The distinction of this time from the above-presented values may be attributed to different counterions (ClO_4^- or OH^-) that accompany the formation of protonated forms and to the existence of equilibrium between the protonated and non-protonated forms of **1**. The increase in the fluorescence lifetimes **2** and **3** in aqueous solution observed after addition of HP-β-CD (16.1 and 15.32 ns) attests to the formation of inclusion complexes also with relatively hydrophilic compounds, which is consistent with the data of NMR spectroscopy.

Scheme 4 describes the processes taking place during the formation of inclusion complexes of **1** with HP-β-CD in the aqueous solution and exciting of fluorescence of **1**.

3.7. Quantum chemical simulation

The goal of our quantum chemical calculations was to consider the energy balance of the protonation/deprotonation processes taking place in the aqueous solution of **1** in the absence and in the presence of HP-β-CD. Simultaneously, the structures of guest, host, and complex molecules were determined and the energies of their formation were calculated. This was done taking into account the fact that the experimentally detected effect of complexation on the spontaneous and photoinduced protonation and the data from NMR spectroscopy attest to the existence of complexes in which the pyridine residue can be located both inside and outside the cavity. In addition, it was meant to find out whether the guest molecule can mechanically move within the cyclodextrin cavity after photoinduced protonation. This process is of interest due to the possibility of designing molecular machines on the basis of this type of inclusion complexes.

In view of the arbitrary choice of the HP-β-CD structure (see Section 2) and of the fact that in calculations of the effect of hydration on the protonation of **1**, we restricted ourselves to considering only five water molecules, for the reason outlines below, the obtained results were used for qualitative interpretation of the observed experimental facts and for demonstration of the general direction of substrate motion in the HP-β-CD cavity.

The calculations were carried out by semiempirical PM3 method [8], which we had repeatedly used to calculate the structures and formation energies of the cyclodextrin complexes with a variety of guests. Although the complexes of cyclodextrins are formed in aqueous solutions, the calculations for isolated complexes formed by hydrophobic molecules with cyclodextrins gave quite realistic results [14]. Since this study considers the properties of complexes formed by a compound comprising a hydrophilic (pyridine) and a hydrophobic (naphthalene) fragments and the formation of

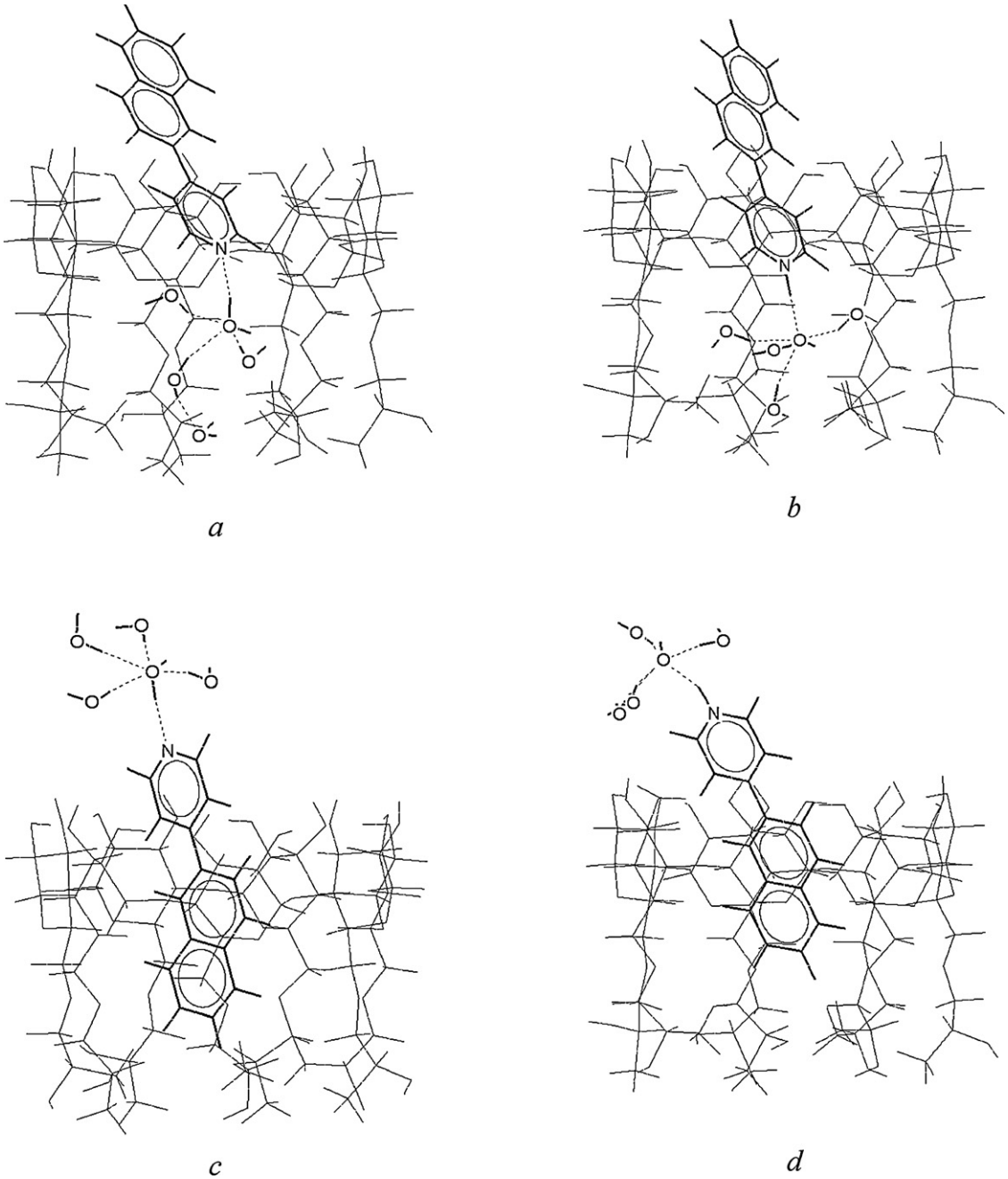

Fig. 7. PM3-calculated structures of complexes (a and c) **1**·5H_2O@HP-β-CD and (b and d) **1**H^+OH^- 4H_2O@HP-β-CD: (a and b) the pyridine residue is inside the HP-β-CD cavity, (c and d) the naphthalene residue is inside the HP-β-CD cavity.

protonated **1** is possible only in the presence of water, the role of water as an essential component was comprehensively investigated. Although PM3 is a semiempirical method, due to the large number of atoms in HP-β-CD and in the complexes, only using this method, one can execute the consecutive calculation procedure: guest molecule (**1**) – host molecule (HP-β-CD) – host–guest inclusion complex. This method is known to be parametrized for deriving realistic structural data and the heats of formation of the molecules, ΔH_f [8]. Thus it is possible to calculate directly the complexation energy and other energy parameters and to estimate the stabilizing or destabilizing effects. The applicability of the method for calculation of hydrogen bonding and proton transfer was considered in a study [15] where it was indicated that for usual distances, for example *l*(N. . .H–O) not exceeding 2.5 Å in hydrogen-bonded complexes, PM3 gives good results.

Comparison of the heats of formation of HP-β-CD of regular structure (C_7 symmetry) and the compound with four primary and three secondary OH groups being replaced shows (Table 3) that the former structure is 12 kcal mol^{-1} energetically more favourable than the latter one. Therefore, subsequently, only the complexes formed by HP-β-CD with C_7 symmetry were considered.

The naphthylpyridine protonation has been studied starting from calculation of the monohydrate **1**·H_2O as only a water molecule can act as the proton donor. The calculation showed that the structure of hydrate **1**·H_2O is found for only one isomer in which the water proton is hydrogen-bonded to the nitrogen atom, $C_{15}H_{11}N\cdots H–OH$, whereas for the other isomer, the $C_{15}H_{11}N^+–H\cdots{}^-OH$ ion pair, i.e., the protonated **1** with the HO^- counter-ion, no local minimum is present in the potential energy

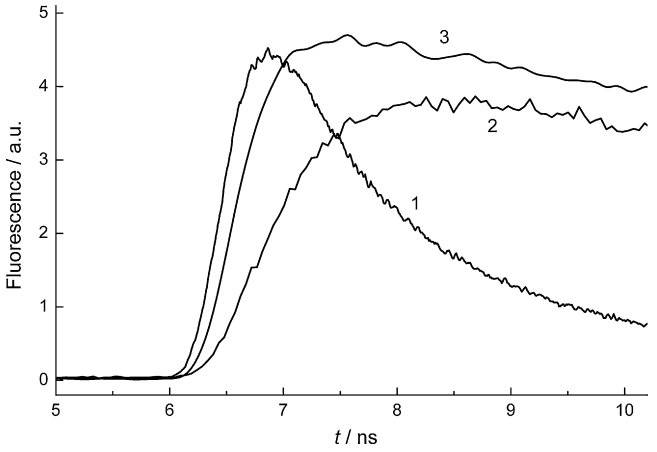

Fig. 8. Initial segments of the fluorescence building-up kinetics of **1** after pulse excitation at 280 nm: (1) in the complex with HP-β-CD, observation at 370 nm (NFF); (2) in the complex with HP-β-CD, observation at 490 nm (PFF); (3) in MeCN, observation at 370 nm (NFF).

surface. This means that spontaneous proton transfer in isolated monohydrate **1**·H_2O is unlikely.

A neutron diffraction study (120 K) of the effect of moisture content on the number of water molecules surrounding β-CD has shown that 11 or 12 water molecules per β-CD molecule are present, of which five or six molecules are located inside the cavity and the other ones are located near the hydrophilic edges of β-CD [16]. The results of molecular dynamic calculations were generally consistent with experimental data: five water molecules were constantly present inside the cavity as the number of water molecules varied from 12 (as in [16]) to 258 [17]; seven water molecules were detected inside the cavity of β-CD surrounded by 827 water molecules [18]. It is significant that water molecules located inside the β-CD cavity were hydrogen-bonded into a closed cluster (cyclic pentamer). In the author's opinion [18], it is the formation of the cluster, which is more hydrophobic than the same number of non-bonded water molecules owing to the higher covalency, that contributes to its positioning inside the hydrophobic cavity.

In view of the facts that (1) the volume of the HP-β-CD cavity is greater than β-CD cavity, (2) no data on the structure of HP-β-CD complexes are available, and (3) the number of water molecules that reside in the cavity is unknown, we first made sure that HP-β-CD can accommodate up to 10 water molecule connected to form two cyclic pentamers. According to calculations, their inclusion energy was – 13.1 kcal mol^{-1}. Therefore, in the absence of the substrate, the HP-β-CD cavity is filled with water molecules, and insertion of the hydrophobic molecule of **1** is accompanied by displacement of some water from the cavity space. Since for geometrical reasons, molecule **1** located in HP-β-CD does not reach the cavity bottom, we also made sure that a water pentamer can be freely accommodated in the remaining space. Therefore, in calculations, we assumed that both naphthylpyridine molecule **1** and water pentamer are located inside the cavity.

To verify the possibility of naphthylpyridine protonation in the presence of five water molecules, we calculated the pentahydrate of **1** and the **1**H^+OH^- ion pair stabilized by four water molecules. It was assumed that, according to the Grotthuss mechanism [19], proton transfer occurs in the $C_{15}H_{11}N\cdots H–OH$ hydrogen bond channel to give $C_{15}H_{11}N^+–H\cdots{}^-OH$, while the remaining four water molecules stabilize the structure with separated charges. The structures of the pentahydrate of **1** and the tetrahydrate of ion pair **1**H^+OH^- found by geometry optimization are presented in Fig. 9.

It can be seen from Fig. 9 that in the pentahydrate, the water molecule located most closely to the nitrogen atom and the hydroxy group in the ion pair are hydrogen-bonded to the four surrounding water molecules, one of which is also hydrogen-bonded to the naphthylpyridine hydrogen atom in the *ortho*-position to the nitrogen atom. The participation of *ortho*-hydrogen to the pyridine nitrogen in hydrogen bonding with the adjacent water molecule was also noted in the protonation of pyridine [12]. It is also seen that due to the negative charge on the hydroxy group, the hydrogen bonds between this group and the surrounding water molecules are markedly shortened.

The calculation showed that the naphthylpyridine – five water molecules system has actually two energy minima of which the structure of pentahydrate **1**·$5H_2O$ is 25.7 kcal mol^{-1} energetically more favourable than the contact ion pair **1**H^+OH^- $4H_2O$ (see Table 3). This difference is in good agreement with the results of calculation of pyridine protonation carried out by a more precise procedure (B3LYP/cc-pVDZ level), according to which pyridine pentahydrate is 28 kcal mol^{-1} is energetically more stable than its protonated form hydrogen-bonded to four water molecules [12]. Thus, protonation in the ground state is endothermic and a fluctuation-type process [19]. This, by the way, accounts for the weak basic properties of pyridine and its derivatives.

Since the energy barrier between the protonated form and the transition state (TS_b) for proton migration between the N and O atoms in the $RN\cdots H^+\cdots OH^-$ system is very low (<1 kcal mol^{-1}) [12], the reverse deprotonation process can occur spontaneously. Note, however, that this is true for a vacuum isolated pyridine pentahydrate, whereas in the aqueous solution bulk, owing to the stabilizing role of the surrounding water, the protonation can be less endothermic and the TS_b barrier can be higher. From this it follows that on irradiation, the light quantum that imparts an energy pulse to the naphthylpyridine molecule, together with bringing the molecule to the excited state S_1, ensures the protonation.

The protonation is facilitated in the excited state owing to the fact that, according to our DFT and TDDFT calculations of the proton affinity (PA) of **1** and **1**H^+ in the ground and excited states with the PBE functional, the PA of **1** in the S_1 state is higher (283.2 kcal mol^{-1}) than in the S_0 ground state (231.3 kcal mol^{-1}). This conclusion is consistent with the published data stating that the higher the PA value of pyridine derivatives, the higher their basicity [20]. The structures obtained by full geometry optimization are shown in Fig. 10.

For complex of **1** with the naphthalene residue in the HP-β-CD cavity:

1·H_2O + 10H_2O@HP-β-CD → **1n**·$5H_2O$@HP-β-CD + 6H_2O $\xrightarrow{h\nu}$

1n*·$5H_2O$@HP-β-CD $\xrightarrow{\tau=1.25ns}$ **1n**·$5H_2O$@HP-β-CD + $h\nu_1$ (375 nm)

1n*·$5H_2O$@HP-β-CD → **1n***H^+OH^-·$4H_2O$@HP-β-CD $\xrightarrow{\tau=17.1ns}$

1nH^+OH^-·$4H_2O$@HP-β-CD + $h\nu_2$ (475 nm)

1nH^+OH^-·$4H_2O$@HP-β-CD → **1n**·$5H_2O$@HP-β-CD

For complex **1** with the pyridine residue in the HP-β-CD cavity:

1·H_2O + 10H_2O@HP-β-CD → **1p**·$5H_2O$@HP-β-CD + 6H_2O $\xrightarrow{h\nu}$

1p*·$5H_2O$@HP-β-CD $\xrightarrow{\tau=4.87ns}$ **1p**·$5H_2O$@HP-β-CD + $h\nu_1$ (375 nm)

1p*·$5H_2O$@HP-β-CD → **1p***H^+OH^-·$4H_2O$@HP-β-CD $\xrightarrow{\tau=6.2ns}$

1pH^+OH^-·$4H_2O$@HP-β-CD + $h\nu_2$ (475 nm)

1pH^+OH^-·$4H_2O$@HP-β-CD → **1p**·$5H_2O$@HP-β-CD

Scheme 4. Formation and fluorescence of inclusion complexes of **1** with HP-β-CD.

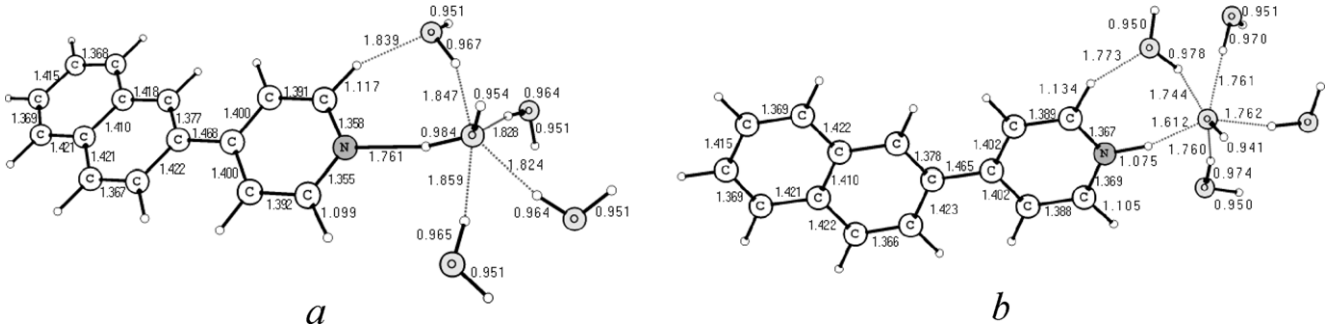

Fig. 9. PM3-optimized structures of: (a) pentahydrate of **1**, μ = 3.21 D, (b) tetrahydrate of protonated **1**, μ = 11.22 D.

It can be seen from Fig. 10 that on passing to the excited state, the molecular geometry changes. Thus on the transition $S_0 \rightarrow S_1$ the structure of **1** becomes flatter, resulting in higher concentration of the electron density in the CNC triad, in particular, the average charge in this fragment increases from $-0.150e$ in the S_0 state to $-0.166e$ in the S_1 state and the bonds are noticeably shortened. In addition, whereas the formation of the protonated $\mathbf{1}H^+$ form results in structure flattening, its transition to the S_1 state induces sharp rotation of both aromatic residues relative to one another, leading to the loss of conjugation between them, to more clear-cut "quinoid" character of the pyridine residue, and to high electron density delocalization in the naphthalene residue of $\mathbf{1}H^+$.

Consider the protonation process of **1** in the presence of HP-β-CD wherein ten water molecules are assumed to be present in the cavity. Since the inclusion energy is -13.0 kcal mol^{-1} and E_{bind} of the pentahydrate is -7.7 kcal mol^{-1} (Table 3), the loss of five water molecules from complex $10H_2O$@HP-β-CD, giving rise to free space in the HP-β-CD cavity for a guest molecule, is endothermic and requires a 5.3 kcal mol^{-1} energy expenditure. However, this energy loss is counterbalanced by inclusion of the naphthylpyridine **1** molecule into the $5H_2O$@HP-β-CD cavity. This energy benefit is 5.3 or 4.0 kcal mol^{-1} for inclusion of **1** by the pyridine and naphthalene fragments, respectively. Hence, insertion of the naphthylpyridine **1** molecule into the HP-β-CD cavity is overally an energetically beneficial process.

The geometry-optimized structures of the pentahydrate of **1** and the tetrahydrate of ion pair $\mathbf{1}H^+OH^-$ inserted into the HP-β-CD cavity are presented in Fig. 7. Note that computer models **1p** $5H_2O$@HP-β-CD (a) and **1p** $H^+OH^-{\cdot}4H_2O$@HP-β-CD (b) reflect more adequately the possible structure of those complexes in which the pyridine fragment is located inside than the models **1n** $5H_2O$@HP-β-CD (c) and **1n** $H^+OH^-{\cdot}4H_2O$@HP-β-CD (d) reflect the structures of complexes in which the pyridine fragment is located outside. The reason is that structures (a) and (b) clearly demonstrate that the number of water molecules that hydrate the pyridine nitrogen atom inside the cavity cannot exceed five. As regards the position of the pyridine fragment outside the cavity (structures (c) and (d)), it is obvious that its hydration is not limited to five water molecules (although their number is actually unknown). However, for estimating the insertion energies, we had to calculate structures with equal numbers of partners.

The energy balance of the interaction of naphthylpyridine **1** molecule with water inside the cavity is shown schematically in Fig. 11 as changes in the formation energy, E_{bind}, of the complexes (Table 3): **1**@HP-β-CD·$5H_2O$, **1**·$5H_2O$@HP-β-CD, and $\mathbf{1}H^+OH^-$ $4H_2O$@HP-β-CD, in which the guest molecule is inserted into the cavity by the pyridine (*1*) and naphthalene (*2*) fragment, respectively. It can be seen from Fig. 11 that in complex **1**@HP-β-CD·$5H_2O$, i.e., without chemical interaction between the guest and water inside the cavity, the location of the naphthalene residue

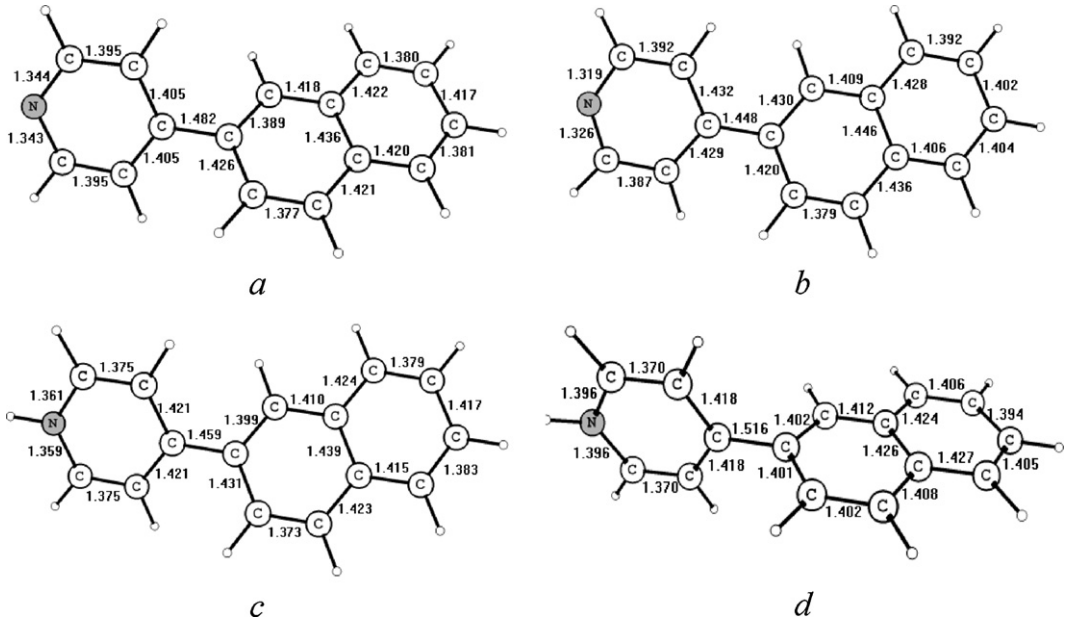

Fig. 10. DFT/PBE-calculated structures of the ground state and TDDFT/PBE-calculated structures of the first excited states: (a) S_0 **1**, ($\angle$ = 34.7°, q_N = –0.225, q_{C_2} = –0.113, q_{C_6} = –0.112 (in *e* charge units); (b) S_1 **1**, ($\angle$ = 12.2°, q_N = –0.192, q_{C_2} = –0.154, q_{C_6} = –0.152, (in *e* charge units); (c) S_0 $\mathbf{1}H^+$, ($\angle$ = –22.4°, PA = 231.3 kcal mol^{-1}; (d) S_1 $\mathbf{1}H^+$, ($\angle$ = –88.4°, PA = 283.2 kcal mol^{-1}.

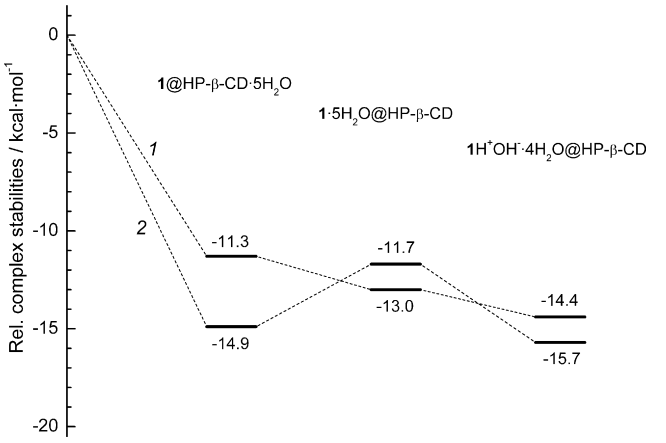

Fig. 11. Evolution of the formation energy of complexes, E_{bind}, for **1**@HP-β-CD·5H_2O, **1**·5H_2O@HP-β-CD, and **1**H^+OH^- 4H_2O@HP-β-CD.

inside the cavity is energetically more favourable than this location of the pyridine residue. This is explained by the fact that before the chemical reaction of the guest with water, it is more preferable for the hydrophobic component to occur inside the cavity. The formation of the pentahydrate stabilizes the complex **1**·5H_2O@HP-β-CD by 1.7 kcal mol^{-1} when the pyridine residue is inside the cavity or destabilizes it if the N·5H_2O group is outside the cavity. Finally, in the ion pair complex **1**H^+OH^- 4H_2O@HP-β-CD, the location of the naphthalene residue inside the cavity is energetically more favourable than this location of the pyridine residue, because the charged N^+–H···$^-$OH·4H_2O fragment is more hydrophilic than the naphthalene fragment, and it is better for the former to occur outside the cavity, i.e., actually in the aqueous environment. Note, however, that the absolute values of the binding energies, E_{bind}, for protonated and non-protonated **1** in the complexes are of the same order of magnitude, and also in any case, the difference between E_{bind} of two types of complexes is not great enough for ruling out the possibility of equilibrium between them. The structures of the complexes of **1**H^+OH^- 4H_2O@HP-β-CD ion pairs calculated by PM3 are shown in Fig. 7.

The deprotonation of the naphthylpyridinium cation located inside the cavity is as follows. Our calculations and published data [12] imply that the ion pair, being less stable as a result of charge separation, is located higher in energy than the hydrate, and four water molecules do not suffice to stabilize it. In the water bulk, the ion pair is stabilized through coordination of a much larger (although unknown and certainly variable) number of water molecules that form a water "coat" around **1**H^+OH^-. However, the hydrophobic nature and the small size of the HP-β-CD cavity accommodating **1**H^+OH^- prevents hydration, and for stabilization, the ion pair is compelled either to leave the cavity or to return the proton back to the aqueous medium surrounding complex **1**H^+OH^-@HP-β-CD. According to spectral data, this actually takes place. In other words, although the formation energy of the complex formed by **1**H^+OH^- with HP-β-CD is somewhat higher than for the neutral **1**·H_2O (see Table 3), it is still insufficient to stabilize the ion pair and it loses the proton.

3.8. Guest motion inside the cyclodextrin cavity after photoinduced protonation

To answer the question whether or not the mechanical motion of the guest after protonation is possible, the distances *L* between the centres of gravity of HP-β-CD and naphthylpyridine placed into the cavity with either the naphthalene or the pyridine residue before and after protonation were calculated. It was assumed that if the *L* value becomes smaller after protonation, then the guest molecule sinks more deeply into the cavity and vice versa. The results are summarized in Table 5.

Table 5
Distance between the centres of gravity of HP-β-CD and naphthylpyridine before and after protonation.

Types of complexes	Distance between the centres of gravity, Å	Δ*L*, Å
1p·5H_2O@HP-β-CD	3.49	0
1pH^+OH^-·4H_2O@HP-β-CD	2.74	−0.75[a]
1n·5H_2O@HP-β-CD	4.61	0
1nH^+OH^-·4H_2O@HP-β-CD	5.41	0.80

[a] Negative Δ*L* means approach of the centres of gravity, i.e., sinking of the guest into the cavity, a positive value means moving of the guest away from the cavity.

It can be seen from Table 5 that in the case where the pyridine residue is located inside the cavity in the complex, then after protonation the *L* value decreases, whereas with the naphthalene residue inside the cavity, *L* increases. In other words, in the former case, the guest sinks inside the cavity upon protonation, whereas in the latter case, it moves away from the cavity (see Fig. 7). Since with allowance for the van der Waals radii of the atoms, the HP-β-CD "basket" is ∼13.5 Å high, the guest travels by quite a noticeable distance within the cavity. This behaviour can be explained by comparing the values and orientations of the dipole moments of HP-β-CD (μ = 1.88 D), pentahydrate of **1**, and ion pair tetrahydrate.

The dipole moment of ion pair tetrahydrate is almost 3 times higher than that of the pentahydrate of **1**. This is a consequence of charge separation. Since the negative end of the dipole of both forms of **1** is directed toward the nitrogen atom, then if it is located inside the HP-β-CD cavity, the orientations of the guest and host dipole moments are approximately antiparallel. Then after protonation the guest should be drawn inside the cavity, because the dipole–dipole attraction increases. When the naphthalene residue occurs inside, the dipoles are parallel to each other. After protonation, due to the sharp growth of the dipole–dipole repulsion, compound **1** would be conversely drawn away from the cavity (see Fig. 7). In conclusion, it should be noted that real mechanical motion of the guest molecule in the latter case after photoinduced protonation can prove to be greater because in our calculations, we are able to take into account only a knowingly minor portion of hydration.

4. Conclusions

Thus, it was found that compounds **1–3** form relatively stable pseudorotaxane complexes with β-CD and HP-β-CD in aqueous solutions and in the crystals. The formation of inclusion complex of **1** with HP-β-CD in solution prevents its protonation, which is a prerequisite for the existence of fluorescence of the non-protonated form of **1** the lifetime of which (1.25 ns) is determined by retarded protonation of **1** in the complex with CD as compared with aqueous solution. These processes are apparently accompanied by light-induced reversible mechanical motion of naphthylpyridine in the cyclodextrin cavity. The established regularities of the photoinduced proton transfer in the pseudorotaxane cyclodextrin complexes can be utilized to design molecular machines using these compounds.

Acknowledgements

This work was supported by the Russian Foundation for Basic Research and the Presidium of the Russian Academy of Sciences. The structural files for quantum chemical calculations were prepared using the program modules developed at the Photochemistry Centre of the Russian Academy of Sciences within the State Contract

No. 02.523.11.3014. The authors are grateful to Mr. V.Yu. Gak for his help in fluorescence lifetime measurements.

References

[1] R. Casadesus, M. Moreno, J.M. Luch, The photoinduced intramolecular proton transfer in 2-(2′-hydroxyphenyl)-4-methyloxazole embedded in β-cyclodextrin, Chem. Phys. Lett. 356 (2002) 423–430.
[2] V.B. Nazarov, V.G. Avakyan, S.P. Gromov, M.V. Fomina, T.G. Vershinnikova, M.V. Alfimov, Spectral properties and structures of supramolecular complexes of naphthylpyridine with β-cyclodextrin, Russ. Chem. Bull. Int. Ed. 53 (2004) 2525–2531.
[3] V.B. Nazarov, V.G. Avakyan, S.P. Gromov, M.V. Fomina, T.G. Vershinnikova, V.Yu. Rudyak, M.V. Alfimov, Pseudorotaxane complexes of naphthylpyridines and naphthylbipyridyl with β-cyclodextrin and hydroxypropyl-β-cyclodextrin, Russ. Chem. Bull. Int. Ed. 56 (2007) 281–289.
[4] S.P. Gromov, M.V. Fomina, Reactions of isoquinoline derivatives with pyridinium salts yielding 4-naphthylpyridines, Russ. Chem. Bull. Int. Ed. 53 (2004) 901–905.
[5] SHELXTL-Plus, Version 5. 10, Bruker AXS Inc., Madison, Wisconsin (USA), 1997.
[6] C. Frassineti, S. Ghelli, P. Gans, A. Sabatini, M.S. Moruzzi, A. Vacca, Nuclear magnetic resonance as a tool for determining protonation constants of natural polyprotic bases in solution, Anal. Biochem. 231 (1995) 374–382.
[7] T. Medinger, F. Wilkinson, Mechanism of fluorescence quenching in solution. Part 1 – Quenching by bromobenzene, Trans. Faraday Soc. 61 (1965) 620–630.
[8] J.J.P. Stewart, Optimization of parameters for semiempirical methods. 1. Method, J. Comput. Chem. 10 (1989) 209–220.
[9] D.N. Laikov, Y.A. Ustynyuk, PRIRODA-04: a quantum-chemical program suite. New possibilities in the study of molecular systems with the application of parallel computing, Russ. Chem. Bull. Int. Ed. 54 (2005) 820–826.
[10] C.W. Yong, C. Washington, W. Smith, Structural behaviour of 2-hydroxypropyl-β-cyclodextrin in water: molecular dynamics simulation studies, Pharm. Res. 25 (2008) 1092–1099.
[11] H.-J. Schneider, F. Hacket, V. Rüdiger, H. Ikeda, NMR studies of cyclodextrins and cyclodextrin complexes, Chem. Rev. 98 (1998) 1755–1785.
[12] M.C. Sicilia, A. Nino, C. Munoz-Caro, Mechanism of pyridine protonation in water clusters of increasing size, J. Phys. Chem. A. 109 (2005) 8341–8347.
[13] M.S. Henry, M.Z. Hoffman, Fluorescence from 2 2′-bipyridine. Evidence for covalent hydrate formation, J. Am. Chem. Soc. 99 (1977) 5201–5203.
[14] V.B. Nazarov, V.G. Avakyan, M.V. Alfimov, Structure and luminescence properties of the inclusion complexes of arenes in cyclodextrins, Rossiiskie Nanotekhnologii 2 (2007) 68–82 [in Russian].
[15] B. Kallies, R. Mitzner, The ability of the semiempirical PM3 method to model proton transfer reactions in symmetric hydrogen bonded systems, J. Mol. Model. 1 (1995) 68–78.
[16] T. Steiner, G. Koellner, Crystalline β-cyclodextrin hydrate at various humidities: fast, continuous, and reversible dehydration studied by X-ray-diffraction, J. Am. Chem. Soc. 116 (1994) 5122–5128.
[17] R.G. Winkler, S. Fioravanti, G. Ciccotti, C. Margheritis, M. Villa, Hydration of β-cyclodextrin: a molecular dynamics simulation study, J. Comput. – Aided Mol. Des. 14 (2000) 659–667.
[18] L. Lawtrakul, H. Viernstein, P. Wolschann, Molecular dynamics simulations of β-cyclodextrin in aqueous solution, Int. J. Pharm. 256 (2003) 33–41.
[19] D. Marx, Proton transfer 200 years after von Grotthuss: insights from ab initio simulations, ChemPhysChem. 7 (2006) 1848–1870.
[20] E.M. Arnett, B. Chawa, L. Bell, M. Tagepera, W. Henre, R.W. Taft, Solvation and hydrogen bonding of pyridinium ions, J. Am. Chem. Soc. 99 (1977) 5729–5738.